

A Generative Framework for Low-Cost Result Validation of Outsourced Machine Learning Tasks

Abhinav Kumar*, Miguel A. Guirao Aguilera†, Reza Tourani*, Satyajayant Misra†

*Department of Computer Science, Saint Louis University, St. Louis, US

†Department of Computer Science, New Mexico State University, Las Cruces, US

Abstract—The growing popularity of Machine Learning (ML) has led to its deployment in various sensitive domains, which has resulted in significant research focused on ML security and privacy. However, in some applications, such as autonomous driving, integrity verification of the outsourced ML workload is more critical—a facet that has not received much attention. Existing solutions, such as multi-party computation and proof-based systems, impose significant computation overhead, which makes them unfit for real-time applications. We propose *Fides*, a novel framework for real-time validation of outsourced ML workloads. *Fides* features a novel and efficient distillation technique—Greedy Distillation Transfer Learning—that dynamically distills and fine-tunes a space and compute-efficient verification model for verifying the corresponding service model while running inside a trusted execution environment. *Fides* features a client-side attack detection model that uses statistical analysis and divergence measurements to identify, with a high likelihood, if the service model is under attack. *Fides* also offers a re-classification functionality that predicts the original class whenever an attack is identified. We devised a generative adversarial network framework for training the attack detection and re-classification models. The evaluation shows that *Fides* achieves an accuracy of up to 98% for attack detection and 94% for re-classification.

Index Terms—Verifiable computing, result verification, trusted execution environment, machine learning as a service.

I. INTRODUCTION

The increasing popularity of machine learning (ML) applications and the plethora of data generated by smart and connected devices, such as smartphones, Internet of Things devices, and video cameras, has led to the development of sophisticated and complex ML applications, such as autonomous driving and cognitive assistance [1]. However, the challenges of processing such a high volume of data to support real-time applications have led to the development of several edge-computing solutions for autonomous driving [2], healthcare [3], and Augmented/Virtual Reality applications [4].

This motivates inference-based ML-as-a-Service (*i.e.*, MLaaS), in which trusted ML providers deploy their services on third-party edge servers as query-based APIs. These APIs allow the clients to share their data with the third-party servers, which are running ML applications, to provide the processed result. The edge computing trust model differs from the Cloud, primarily due to its distributed and multi-stakeholder nature [5]. Given that any entity may host a third-party server, outsourcing ML applications to the edge ecosystem raises potential privacy and security issues, including model/data inference and Trojan attacks [6]–[12].

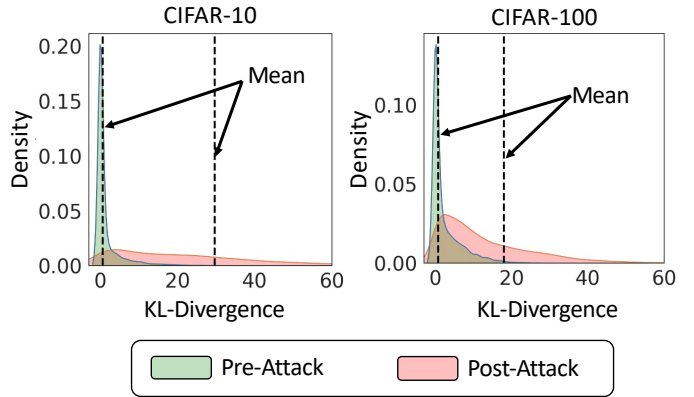


Fig. 1: The KL divergence density distribution between two models, **ResNet50** and **ResNet152** before attack (green) and after attack (red) on **CIFAR-10** and **CIFAR-100** datasets. The KL divergence between the benign models' posterior vectors belongs to a distribution with low mean and variance (green distribution). Performing a prediction-switching attack against one of the models (ResNet152) leads to a significant increase in the distribution's mean and variance (red distribution). We use this identifiable behavior in designing *Fides*. (distributions' tails are truncated for better visualization).

Two of the most pertinent attacks against outsourced ML integrity are Trojan attacks [10], [11] and adversarial example [13], [14]. In Trojan attacks, the attacker partially modifies the neural network using a poisoned dataset to include a set of samples with a pattern trigger, aiming to cause misclassifications when the model observes the pattern trigger. Backdoor attacks can be devised either during model training or on a pre-trained model [8], [10], [11], [15]. An adversarial attack (*i.e.*, adversarial example) exploits the inherent vulnerabilities of neural networks to achieve misclassifications post-training. These attacks are input-specific in that each input data should be individually perturbed to cause a misclassification.

The existing techniques for preserving the integrity of outsourced computation use cryptosystems, such as multi-party computation [16]–[19], proof-based systems [20]–[22], and homomorphic encryption [22]–[25]. A few initiatives have built frameworks using a Trusted Execution Environment (TEE) to offload parts of the ML applications [26], [27]. Despite their merits, these solutions are often computationally expensive, impose significant latency overhead, or do not scale with the complexity of the evolving ML models. Thus, making them impractical for real-time and latency-sensitive applications. Some solutions utilize multiple models in the

form of redundant computing or majority voting [28], [29]. Redundant computing techniques, however, require higher degrees of redundancy to achieve stricter integrity guarantees, which leads to significantly higher computational overhead. Moreover, redundant computing techniques are built on the presumption, that the only relevant part of a model’s output is the predicted class, which is not true. *The model’s posterior vector provides information about the learned knowledge representation through the probabilities assigned to the minority classes.* This insight has been utilized in knowledge distillation to train higher accuracy and fidelity compressed versions of cumbersome models [30]. We believe the same insight can be used to study the impact of an adversary on two models trained on identical distribution. Figure 1 shows the density distribution of Kullback–Leibler (KL) divergence between two models (ResNet50 and ResNet152) and the drastic change in the distribution when an adversary manipulates the prediction generated by one of the models (ResNet152). We will further analyze the impact of an adversary on the divergence trends (Section IV) and use it to create a result validation framework.

Our Framework: To cope with the attacks that target inference integrity, we propose Fides¹. In a nutshell, Fides validates the integrity of the outsourced ML task by securely running a special-purpose *verification model*. This model is constructed through knowledge distillation, guaranteeing that the knowledge representation of the verification model closely approximates that of the service model. Fides comprises two primary components. The first one is a resource-efficient model distillation technique—Greedy Distillation Transfer Learning (GDTL)—which generates a customized verification model for a given service model. GDTL distills the knowledge of the service model into the verification model by incrementally unfreezing and fine-tuning the last layers of the model. This leads to only a few layers being distilled at a time, which makes it suitable for resource-constraint and TEE-based private training paradigms [29], [31]. The second component is a novel generative framework for training a client-side attack detection model that uses posterior vectors of the service and verification models, alongside their divergences, on a given input to detect a potential attack. Our framework also trains an attack re-classification model, aiming to predict the correct result of the outsourced task by learning a typical adversary’s goal and behavior in the system under attack.

We evaluate Fides’ performance using three benchmark datasets, including CIFAR-10, CIFAR-100, and ImageNet, across three neural network architectures and further assess its computational overhead on multiple constrained devices. Finally, we compare Fides with Slalom [26] and Chiron [32], and show that Fides achieves $4.8 \times$ – $26.4 \times$ and $1.7 \times$ – $25.7 \times$ speed-up to Slalom and Chiron, respectively.

The novel **contributions** of Fides are as follows:

(i) We propose Fides—a framework for result validation of outsourced ML task using an efficient verification model running on a TEE to corroborate the results of the service model. This

makes Fides a perfect candidate for real-time applications, such as autonomous driving, and medical imaging.

(ii) In designing Fides, we propose a greedy distillation transfer learning (GDTL) technique for training the verification model, aiming to reduce the distillation’s overhead by incrementally unfreezing layers of the verification model for fine-tuning to achieve the desired accuracy.

(iii) We introduce two client-side shallow neural networks for detecting and resolving adversarial attacks, with negligible computation overhead. We propose a generative framework for effective training of these models.

(iv) We systematically assess Fides using major benchmark datasets of varying complexity and number of detection classes on three architecturally different deep neural networks: namely ResNet [33], DenseNet [34], and EfficientNet [35]. Our results show that Fides outperforms existing solutions in terms of computation complexity while achieving high attack detection and remediation accuracy.

Section II presents the background. We present our threat model, assumptions, and attack modeling in Section III. We then share the observation that motivated our design in Section IV followed by the design of Fides in Section V. Section VI presents our experimental insights. Section VII includes the related work Section VIII shares our conclusion.

II. BACKGROUND

In this section, we introduce the concepts relevant to our work, including a trusted execution environment, ML compression techniques, and divergence-based similarity measures.

A. Trusted Execution Environments

A Trusted Execution Environment (TEE) is an isolated processing environment in which each application is allocated a region of memory, called an enclave, which is protected even from processes running at higher privilege levels [36], [37]. The TEE guarantees the integrity of the run-time states, the confidentiality of the code and data stored on persistent memory, and the authenticity of the executed code and its correct execution via remote attestation between the data owner and the secure enclave. The two common TEE implementations are Intel SGX [38] and ARM TrustZone [39].

B. Model Compression

Model Quantization [40] is a strategy for model compression and inference process acceleration. Quantization reduces the precision of the model’s weight, gradient, or activation values by converting floating point numbers to lower precision integer numbers [41]. Thus, reducing the storage needed for the model and speeding up the inference task [42]. The two primary quantization strategies include post-training quantization, where the weights of a trained model will be compressed (*e.g.*, 32-bit float to 8-bit integer), and quantization-aware training, in which the model’s weight and gradients are quantized during the training process [43].

Knowledge distillation (KD) [30] is a machine learning technique for transferring knowledge from a complex neural

¹*Fides* is the goddess of trust according to Roman mythology.

network(s) (*i.e.*, teacher model(s)) to a single model (*i.e.*, student model), aimed at model compression, robustness, and performance enhancement [44]–[46]. The distillation process entails training the student model using the output feature maps of the teacher model, *i.e.*, soft labels, and their corresponding true labels. The distilled models tend to be more robust against adversarial attacks when compared with their teacher models [47], [48]. Defensive distillation [49] is a technique that helps in reducing the effectiveness of the adversarial example attacks against DNNs.

C. Similarity Measures

Divergence-based similarity measures are statistical techniques to assess the similarity of a probability distribution (P) with respect to the reference probability distribution (Q). We review the Jeffreys' divergence (JD) and Wasserstein distance.

Jeffreys' Divergence. The JD is the bounded symmetrization of the Kullback–Leibler divergence (KLD), which is used to quantify the similarity between two probability distributions P and Q . Unlike KLD, the JD distance represents a normalized score that is symmetric, *i.e.*, $D_J(P \parallel Q) = D_J(Q \parallel P)$ and can be calculated as:

$$D_J(P \parallel Q) = \frac{1}{2} D_{KL}(P \parallel Q) + \frac{1}{2} D_{KL}(Q \parallel P),$$

where $D_{KL}(P \parallel Q)$ is the KLD between P and Q . JD provides a smoothed and normalized score compared to KLD.

Wasserstein-1 Metric. Wasserstein-1 distance is a measure of the distance between two probability distributions. Informally, the Wasserstein distance can be interpreted as the minimum energy cost of moving the mass from x to y to transform probability distribution P to Q . Wasserstein-1 metric (D_W^1) between cumulative distribution functions P and Q is defined as the infimum, taken over the set of all joint distribution $\Gamma(P, Q)$. Thus, the Wasserstein-1 distance between P and Q ($D_W^1(P, Q)$) is:

$$D_W^1(P, Q) = \inf_{\gamma \in \Gamma(P, Q)} \mathbb{E}_{(x, y) \sim \gamma} [|x - y|].$$

III. MODELS AND ASSUMPTIONS

In this section, we first describe our system model and then formalize our threat model and discuss security assumptions. Our system comprises edge servers, ML service providers, and clients. Service providers offer a range of resource-intensive machine learning services, such as image annotation or video analytics, which require input data from the clients. Given the complex nature of the computation load and the need for real-time computation of these services (*e.g.*, autonomous driving, multi-player gaming, and traffic monitoring), clients outsource their services to the edge server instead of using the distant Cloud. We envision a subset of the servers to be equipped with low-end trusted hardware like Intel SGX or AMD TrustZone.

A. Threat Model

Attacks against computation outsourcing may target confidentiality, integrity, availability, and privacy. Among all, we focus on threats to integrity. Thus, the primary objective of

Fides is to provide correctness verifiability for the output of the outsourced ML task. More specifically, given an ML task and its input data, the goal is to enable the client to assess the reliability of the result and infer, with high probability, the trustworthiness of the executed service.

We formalize our threat model by introducing a *security game*, in which the adversary \mathcal{A} has to generate malicious predictions and deceive the challenger \mathcal{C} into believing that the generated predictions belong to the universe \mathcal{U} of benign input, prediction pairs.

Detection Game The game utilizes a data universe $\mathcal{U} := \{(x_i, F_\theta(x_i))\}_{i=1}^N$, where $F_\theta : x_i \rightarrow [0, 1]^n$. The function F_θ is realized through a machine learning model and trained using algorithm τ_F . While both the challenger \mathcal{C} and Adversary \mathcal{A} have complete knowledge of input distribution \mathbb{D} , trained model F_θ , training algorithm τ_F , and attack detection algorithm τ_F^D , the challenger has no knowledge of the attack algorithm τ_F^A used by adversary.

- 1) The challenger samples the dataset $\mathcal{D} \subseteq \mathbb{D}$ and trains model $F_\theta \leftarrow \tau_F(\mathcal{D})$, where $F_\theta : x_{i=1}^N \rightarrow y_{i=1}^N$ and $(x_i, y_i)_{i=1}^N \in \mathcal{U}$.
- 2) The challenger gives adversary a white-box access to F_θ .
- 3) The adversary runs $\tau_F^A : (x, y) \rightarrow \tilde{y}$, such that $(x, \tilde{y}) \cap \mathcal{U} = \emptyset$, and returns $\{(x, y), (x, \tilde{y})\}$.
- 4) The challenger generates a guess $z \in \{y, \tilde{y}\}$ by running $\tau_F^D(\{y, \tilde{y}\}; x, F_\theta)$.
- 5) The adversary wins if $(x, z) \notin \mathcal{U}$.

The adversary can implement τ_F^A in several different ways, including orchestrating Trojan attacks on image or text classification data [10], [11], performing attacks on the input image in the form of adversarial perturbation [13], [14], or leveraging their access to the model and directly modifies the model weights or prediction vector.

We do not impose any restriction on the adversary's access to the service model, which is running in the insecure region of the general purpose processor. The adversary has complete knowledge of the architecture and parameters of the service model. We assume that the adversary is aware of the deployed defense mechanism or its components within a trusted enclave but does not have access to any computations taking place inside the enclave and can use its knowledge of the defense algorithm τ_F^D to orchestrate targeted attacks.

B. Attack Modeling

The primary outcome of the attack we consider in this work is the integrity violation of the outsourced ML task. To achieve this goal, the adversary can use different techniques. In what follows, we discuss three prominent attack orchestration techniques and implement them in our evaluation. All the attacks take place at the edge server, with the attacker deciding which of the different attacks to execute. The attacker's goal is to have the service model classify an input with a wrong label. We note that while the adversary can completely control the execution of the service model, the adversary cannot interrupt the verification model as it runs in the secure enclave upon the client's request. We start with an attacker with minimal

capability and knowledge and gradually increase the attack sophistication. We implemented these attacks and tested Fides against them.

Prediction Switching Attacks. In the following attack methodology, the adversary only targets the posterior vector of the deployed machine learning model and modifies it directly, aiming to cause an incorrect prediction. We call this attack *naive prediction switching attack* if the attacker modifies or generates the predictions arbitrarily, without any attempt to avoid the detection mechanism. With the knowledge of a detection mechanism, the adversary may deploy different strategies, such as averaging the two highest probability values p_1 and p_2 ($\mu = \frac{p_1+p_2}{2}$) to switch the prediction by assigning $\mu + \epsilon$ to the second class (*i.e.*, wrong prediction) and $\mu - \epsilon$ to the first class (*i.e.*, true prediction), using a small ϵ value, *e.g.*, 0.01% of μ . Alternatively, the adversary trains its own verification model and uses it to minimize the distance between the forged incorrect prediction and the actual prediction of the service model. We call these *advanced prediction switching attacks*.

Well-known Attacks. The adversary can use popular backdoor or adversarial sampling techniques to modify the predictions. For our evaluation, we consider the following attacks:

Fast Gradient Sign Method (FGSM) [50] perturbations are crafted by calculating the loss between the prediction and the true label. Using the calculated loss, FGSM creates a max-norm constrained (ϵ) perturbation. Given image x , the adversarial image x^{adv} can be calculated as $x^{adv} = x + \epsilon \times \text{SIGN}(\nabla_x J(\theta, x, y_{true}))$.

Projected Gradient Descent (PGD) [51] acts as iterative extension of FGSM. The adversarial image is crafted by repeatedly adding perturbation, guided using the loss between the prediction and the target class. Each step of adversarial image generation can be formulated as $x_{N+1}^{adv} = \text{Clip}_{X, \epsilon}(x_N^{adv} + \text{SIGN}(\nabla_x J(\theta, x, y_{target})))$, where $x_0^{adv} = x$.

Trojan Attacks: This attack is conducted using the service model in a white-box setting. In the context of our work, the adversary can train the service model with a poisoned dataset containing trigger embedded images [52] [53]. Alternatively, the adversary adds more layers to the service model as a Trojan module and trains it using the poisoned data [8], which gets triggered when the input image contains the embedded trigger.

IV. OBSERVATION

In this section, we will discuss our findings regarding the disparities between two models, which were trained on datasets with similar distributions, where one is subjected to an attack that causes mispredictions. The insights drawn from these observations, coupled with the evident trend we have identified, lay the foundation for the design of Fides.

Consider two neural networks, F_θ^1 and F_θ^2 , where F_θ^1 is trained on the data distribution \mathcal{D} and F_θ^2 is trained using an algorithm that distils the knowledge of F_θ^1 into F_θ^2 . Even though F_θ^2 distills the knowledge of F_θ^1 , they have differences in the learned decision boundaries. We speculate

that orchestrating prediction-switching attacks, *i.e.*, adversarial attacks in which malicious actors modify the posterior vectors of a model during inference, on only one of the models will have a noticeable impact on the divergence between the posterior vectors of F_θ^1 and F_θ^2 . If this is true, the question that arises is: *Do such disturbances to the divergence values create distinctive trends, and can we utilize them for attack identification?* As such, we analyze the divergence density distribution of F_θ^1 and F_θ^2 —both before and after conducting a prediction-switching attack against F_θ^1 . In comparing the divergence trends, *i.e.*, $D(F_\theta^1(x), F_\theta^2(x))$, we consider the following cases:

- **Natural Agreement (Case A):** $\text{argmax}(F_\theta^1(x)) = \text{argmax}(F_\theta^2(x))$ prior to any adversarial modifications to the prediction.
- **Natural Disagreement (Case B) :** $\text{argmax}(F_\theta^1(x)) \neq \text{argmax}(F_\theta^2(x))$ prior to any adversarial modifications to the prediction.

Using these two cases, we aim to recognize identifiable patterns between naturally occurring disagreements and those resulting from malicious actions. In our analysis, we employ three datasets: CIFAR-10, CIFAR-100, and ImageNet, and three architectures: ResNet, DenseNet, and EfficientNet (more details in Section VI). For assessing divergence, we use Jeffreys' Divergence and Wasserstein-1 measures. Figure 2 shows the JD distributions between the output of the two models across all datasets and architectures. We identified evident trends between pre-attack and post-attack JD distributions:

Trend 1: First, let's consider Case A, where both models naturally agree on the predictions. The results reveal that in typical conditions when neither of the models is under attack, the similarity between their output distributions leads to a concentrated JD distribution. This distribution exhibits small standard deviation and mean values, as depicted by the green curve in Case A. In contrast, when one of the models is subjected to an attack, the JD distribution undergoes a significant transformation, with a sharp increase in both the mean and standard deviation values, illustrated by the red curve in Case A.

Trend 2: Next, let's consider Case B, where the two models naturally exhibit disagreements. This occurs when only one of the models predicts the true label, or when both predictions differ from the true label and each other. In this scenario, we observe a contrasting phenomenon. Specifically, when the system is not under attack, the differences between the outputs of the two models result in a wide JD distribution with a relatively larger standard deviation and mean values, as shown by the green curves in Case B. On the contrary, the attack leads to a narrow JD distribution with smaller standard deviations and mean values, as indicated by the red curves in Case B.

The trends we have identified, which remained consistent across various architectures and datasets, and the observations from Figure 2 are the key supporting elements that empirically validate our intuition behind the impact of an attack on the similarity of two probability distributions. In particular, the results confirm that *if the two models agree with each other,*

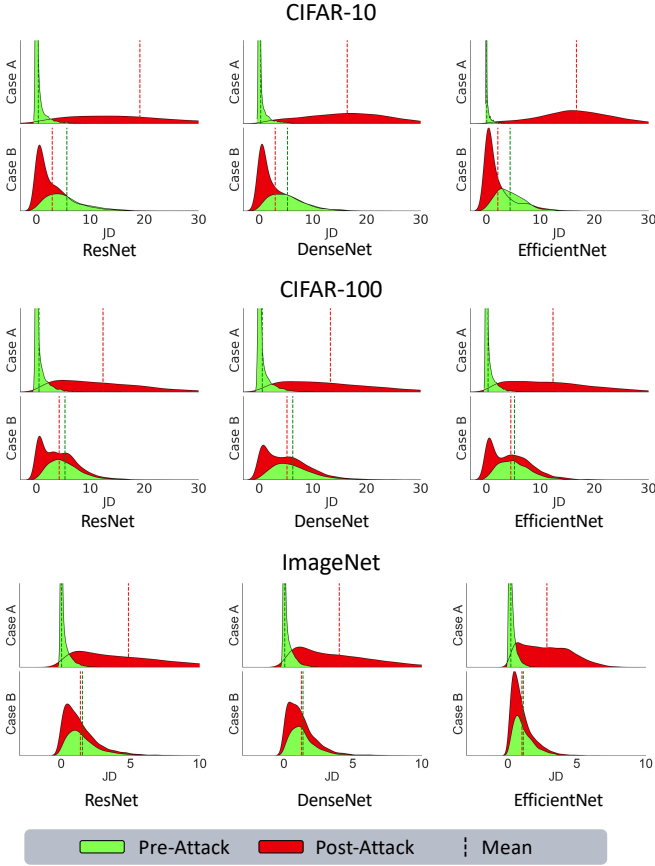


Fig. 2: The JD measurements of two models. Evidently, the attack leads to an increase in the divergence value, whereas in Case B (disagreement), the attack decreases the divergence value. Thus, validating our reasoning for divergence’s role in attack detection.

an attack will lead to an increase in the mean and standard deviation of the divergence, resulting in a wide distribution. In contrast, when the two models have natural disagreements, the attack decreases the mean and standard deviation of the divergence distribution, leading to a narrow distribution. We also measured the similarity of the two models using the Wasserstein-1 metric to show independence from any particular similarity measure. Our analysis shows similar trends in different value ranges (refer to Table III and Table IV in Appendix A). The observations shown above, however, pose a major challenge. There are overlaps between the pre-attack and post-attack distributions across all cases. Moreover, increasing the complexity of the dataset and the dimensionality of the output vector leads to an increase in the overlap. This growing overlap and complexity serve as indicators of a more complex decision boundary for the attack discrimination task, which can potentially be realized through a neural network. We will address this challenge in our design (Section V-B).

V. DESIGN OF FIDES

In a nutshell (refer to Figure 3), the process of Fides starts with a service provider preparing the service package (§ V-A),

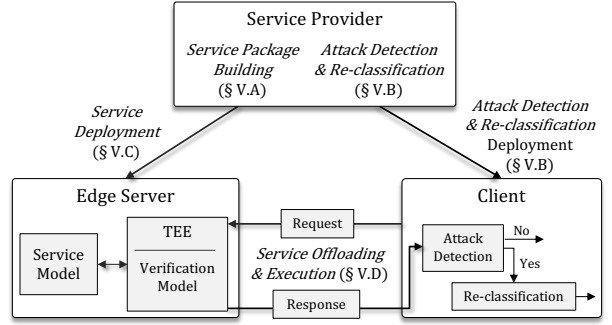


Fig. 3: In Fides, the provider builds the service package (§ V-A) and the attack detection and re-classification pipeline (§ V-B) for deployment on the server (§ V-C) and the client, respectively. The client then offloads the service execution to the edge server and verifies the result using the attack detection pipeline (§ V-D).

including the ML application, *i.e.*, service model, and its verification component, *i.e.*, verification model, for deployment on the edge servers (the server-side component). The service provider also builds an attack detection and re-classification pipeline, that includes two neural networks (§ V-B), one for attack detection and a second for re-classification. In training the attack detection and re-classification models, the provider uses a generative adversarial network approach. The service deployment process involves loading the service and verification models to a server with which a trust relationship has already been established (§ V-C). After deployment, the server accepts requests for verification from a client. On receiving a client’s request, the server runs the verification model inside the secure enclave and the service model in the unprotected region of the processor and returns both outputs to the client (§ V-D). Finally, the client runs Fides’ detection and re-classification functionalities (the client-side component) to identify a potential attack and rectify the outcome of the outsourced service as needed. Without loss of generality, we use Intel SGX as the TEE in our implementation reference and explain details using SGX terminology.

A. Service Package Building

A service package includes two components—the application (*i.e.*, service model) and a verification tool (*i.e.*, verification model), which is a small ML model for the verification of its corresponding service model. As shown in Figure 4, service package development is a two-step process in which the provider first trains its service model, *e.g.*, image classification, and then dynamically re-train layers of the verification model using the fully trained service model.

As per Algorithm 1, the service building process takes an untrained service model (F_S), an independently pre-trained verification model (F_V), the privately owned training set (\mathbb{D}_T^{Priv}), and a set of hyper-parameters (λ and α). Upon completion, it returns the fully trained service (F_S) and verification (F_V) models. Training the service model follows the standard training process using \mathbb{D}_T^{Priv} with the defined loss function for as many epochs as required (Lines 1-3). The verification model

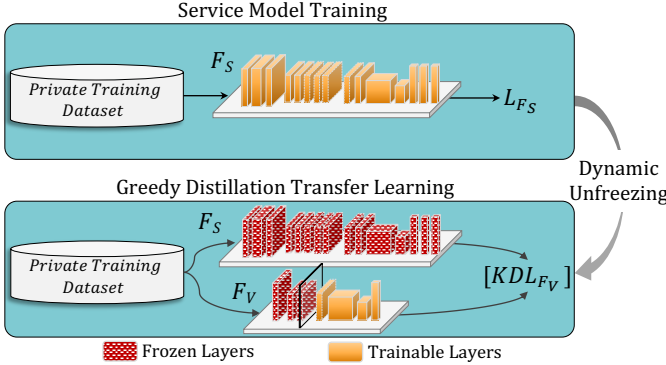


Fig. 4: In service package building, the provider trains the service model and uses it to run the greedy distillation transfer learning process, which builds the customized compressed verification model.

is a distilled and smaller version of the service model, so it renders minimal computation overhead when deployed into the edge server's enclave. To reduce the cost of knowledge distillation, we propose *Greedy Distillation Transfer Learning* (GDTL), a distillation technique that results in a time-efficient procedure for training the small verification model.

The GDTL process takes a pre-trained model that is significantly smaller as compared to the service model and adaptively unfreezes the layers that require re-training and fine-tuning. More specifically, GDTL first splits the verification model starting from its last layer (Line 8). Given the model split, GDTL runs F_S and F_V on \mathbb{D}_T^{Priv} to obtain the soft labels of the service model and the partially trained verification model (Lines 8-10). In Line 10, GDTL calculates the knowledge distillation loss (*i.e.*, KDL) of these values and the one-hot encoding (τ) of the labels (Line 5). Note that the weight of the average (α) changes over time. GDTL starts with a larger α value, giving more weight to the teacher model, and then adaptively decreases it over time, giving higher weight to service true label. The rationale for adaptively changing α is to initially guide the model towards the service model and then decrease it for it to improve over samples the teacher model is providing incorrect prediction. GDTL then uses the loss value and the stochastic gradient descent method to update the trainable layers (Line 11) using \mathbb{D}_T^{Priv} .

Each training iteration, GDTL compares the accuracy and precision of the partially fine-tuned verification model with the service model. If the verification model's accuracy is higher than the λ factor of the service model's accuracy, the GDTL process stops training F_V (Lines 7). Otherwise, GDTL dynamically unfreezes another layer of the verification model for fine-tuning (Line 12). In essence, the GDTL process gradually splits the model from the last layer towards the first and continuously re-trains and fine-tunes the trainable layers. We note that λ is a hyper-parameter that the provider adjusts based on various factors like its available computing resources and the desired verification accuracy. A λ value closer to 1 results in a high-accuracy verification model but requires more fine-tuning steps. Our initial assessment (Figure 5) shows that GDTL outperforms standard distillation

Algorithm 1: Service Package Development

Input: F_S (untrained), F_V (public pre-trained), \mathbb{D}_T^{Priv} , $\lambda \in [0, 1]$, $\alpha \in [0, 1]$.

Output: $\langle F_S, F_V \rangle$.

Service Model Training:

- 1 **for** *number of the training epochs* **do**
- 2 Use stochastic gradient descent to update F_S on: $\mathcal{L}_{F_S}(F_S(x_i), y_i), \forall (x_i, y_i) \in \mathbb{D}_T^{Priv}$
- 3 **Store** F_S $\triangleright F_S$ is the fully-trained Service model.
- 4 $\bullet_{j=1}^n F_V \leftarrow F_{V1} \bullet F_{V2} \bullet \dots \bullet F_{Vn}$

Distillation-based Fine-tuning:

- 5 $l \leftarrow n$ \triangleright Set the cut-layer to the last layer of F_V .
- 6 $\tau \leftarrow$ ONE HOT ENCODING of data label (y_i).
- 7 **while** $(l \geq 1 \ \&\& \text{ACC}(F_S) \leq \lambda * \text{ACC}(F_V))$ **do**
- 8 $\{ \bullet_{j=1}^{l-1} F_{Vn}, \bullet_{j=l}^n F_{Vn} \} \leftarrow \text{ML-SPLIT}(F_V, l)$
- 9 **for** $(\forall (x_i, y_i) \in \mathbb{D}_T^{Priv})$ **do**
- 10 $KDL(F_S(x), F_V(x), \tau, T) =$
 $- \alpha \mathbb{E}_{F_S(x)} \left[\log \left(\frac{F_V(x)}{T} \right) \right]$
 $- (1 - \alpha) \mathbb{E}_{\tau} \left[\log \left(F_V(x) \right) \right]$
- 11 Use stochastic gradient descent to update
 $\bullet_{j=l}^n F_V$ on: $KDL(F_S(x), F_V(x), \tau)$,
where gradients = gradients $\times T^2$
- 12 Unfreeze $(\bullet_{j=l}^n F_V)$ by adjusting the cut layer in
 $F_V : l \leftarrow l - 1$.
- 13 **QUANTIZE**(F_V) \triangleright Dynamic-range quantization.
- 14 **Return** $\langle F_S, F_V \rangle$ \triangleright Fully-trained Service model
and fine-tuned distilled verification model.

and fine-tuning in terms of accuracy and is comparable to fine-tuning in terms of per-epoch execution time. GDTL also reduces the difficulty of finding suitable regularization, which is the primary reason behind the lower accuracy of classical knowledge distillation [54].

For further compression, GDTL applies model quantization as a common technique for approximating a neural network that uses floating-point numbers using a neural network of lower bit-width numbers. Among all, in Fides, we used dynamic range quantization (Line 13), which is a post-training approach that does not need additional model re-training and fine-tuning. Dynamic range quantization converts 32-bit floating point numbers into 8-bit integers, with the resultant model running using floating point operations. At the end of this process, the service package is completed. It should be pointed out that the design of the distillation algorithm relies on an underlying assumption that pre-trained weights utilized are trusted. Violation of this assumption can lead to vulnerabilities [15], which are out of the scope of this work.

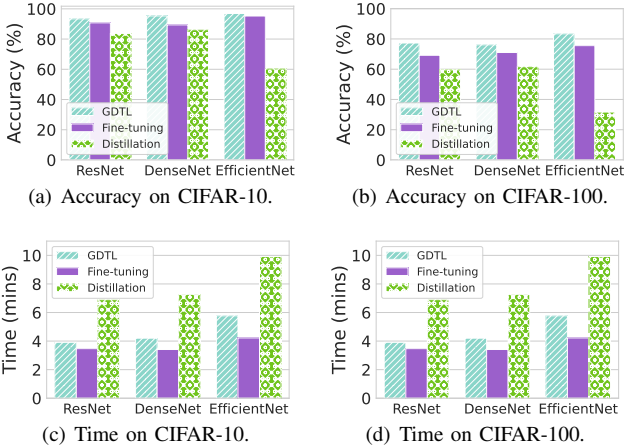


Fig. 5: The performance comparison between GDTL, distilling from scratch (Distillation), and fine-tuning (Transfer Learning) across multiple datasets and architectures. The results show the accuracy and per epoch time for all approaches showcasing how GDTL outperforms other approaches while being resource-efficient.

B. Generative Attack Detection and Re-classification Training

Before elaborating on the design of Fides’ attack detection and re-classification models, we discuss the reasoning behind the impact of attacks that cause misprediction, which serves as the basis of our detection and re-classification models. Intuitively, when not under attack, the outcome of the service and verification models will be almost identical, which results in similar probability distributions and a lower divergence between them. In contrast, an attack that causes different class labels between the service and verification models will lead to a more significant divergence between the two probability distributions. It is evident that the divergence between the service and verification models’ probability distributions reveals statistical information, which is essential for attack detection. We use this analytical reasoning to utilize the differences in the relative divergence as features to assist attack detection.

For attack detection, a naive approach would be using the resultant divergence of the two probability distributions to set a fixed attack detection threshold. However, manually setting a threshold is not effective since (i) the threshold is model and data-specific, and (ii) the attack detection decision boundary is non-linear, for which a linear threshold will be ineffective. Supervised learning algorithms can effectively learn such non-linear decision boundaries and improve the detection accuracy. However, these algorithms will be ineffective in detecting variations of known attacks or attacks that are outside the training dataset. Hence, we used a GAN framework for training Fides’ detection and re-classification models, allowing them to learn the divergence ranges of normal and under-attack scenarios. Using GAN results in a more exhaustive exploration of the search space of representative attacks.

The correlation of the outputs of the service and verification models will result in five possible cases. Case *C1* is when both models agree with the ground truth. Case *C2* is when only the service model agrees with the ground truth while

Case *C3* represents those instances where only the verification model agrees with the ground truth. For Case *C4* both models make two different incorrect predictions. In Case *C5*, both models make the same incorrect prediction, *i.e.*, disagree with the ground truth but happen to agree with each other. These cases are accounted for in our GAN framework to train the attack re-classification model. Note that the re-classification model is a five-class classifier, which returns one of these cases regardless of the number of classes in the service model.

GAN-based Attack Detection and Re-classification. We formalize the training of Fides’ attack detection model (\mathcal{D}) and the attack generator model (\mathcal{G}) as a min-max game. The generator is an attack crafting neural network, which takes samples from the private dataset (\mathbb{D}_T^{Priv}) and it returns outputs that are different from the service model. The goal of the detection model, *i.e.*, the discriminator, is to differentiate between the output of the service model and the generator model’s crafted outputs. The generative training process simultaneously trains a re-classification model (\mathcal{R}), which aims at correcting the attack’s outcome by reclassifying the output of the service model when under attack.

In training the generator and detection models, we define the objective function of the min-max game as:

$$\begin{aligned} \min_{\mathcal{G}} \max_{\mathcal{D}} V(\mathcal{G}, \mathcal{D}) = & \mathbb{E}_{x \sim p_{data}(x)} \left[\log \left(\mathcal{D}(F_S(x), F_V(x)) \right) \right] \\ & + \mathbb{E}_{x \sim p_{data}(x)} \left[\log \left(1 - \mathcal{D}(\mathcal{G}(x), F_V(x)) \right) \right] \\ & - \mathbb{E}_{x \sim p_{data}(x)} \left[\log \left(1 - \mathcal{G}(x) \right) \right]. \end{aligned}$$

The first and second terms are the cross-entropy between the output of the attack detection model and its true label $\mathcal{Y}_{\mathcal{D}}$ ($\in \{0, 1\}$), where 1 signifies no attack while 0 signifies attack. The third term is the cross-entropy between the generator model’s output and the private data’s true label. Our proposed objective function is different from the conventional generative adversarial networks in two aspects. First, the addition of the third term penalizes the generator model every time its prediction is the same as the true label. Thus, preventing the generator model from converging with the service model. Second, the generator model does not sample any input noise. Instead, it uses samples from the private dataset as input and crafts a malicious output with a wrong label, while mimicking the decision boundary of the service model.

Recall that the generator model takes the samples from the private dataset as input and generates malicious outputs. We define a malicious output to be a prediction that is different from the true label but has a probability distribution similar to a naturally occurring misclassification. To achieve this behavior, we define the generator model’s loss function as:

$$\mathcal{L}_{\mathcal{G}} = -\log \left(\mathcal{D}(\mathcal{G}(x), F_V(x)) \right) - \log \left(1 - \mathcal{G}(x) \right).$$

The first term in $\mathcal{L}_{\mathcal{G}}$ rewards the generator model every time the detector model classifies the output of the generator model as a valid output. The second term rewards the generator model for making predictions that are different from the true labels.

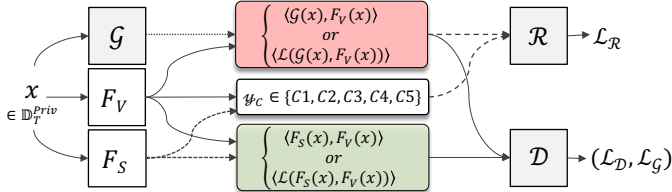


Fig. 6: We formalized the attack detection and subsequent reclassification models as a GAN, in which the attack generator (\mathcal{G}) crafts various attacks to train the attack detection (\mathcal{D}) model in a two-player min-max game. In the process of training \mathcal{G} and \mathcal{D} , the framework simultaneously trains a re-classification model (\mathcal{R}), aiming to correct the outcome of the attack.

The input of the detection model comprises two tuples (Figure 6). The first tuple consists of the outputs of the generator model $\mathcal{G}(x)$ and verification model $(F_V(x))$ alongside their cross-entropy loss $(\mathcal{L}(\mathcal{G}(x), F_V(x)))$. The second tuple consists of the outputs of the service model $(F_S(x))$ and verification model $(F_V(x))$ alongside their cross-entropy loss $(\mathcal{L}(F_S(x), F_V(x)))$. We define the loss function of the detection model as the binary cross-entropy between the model's output and its true label:

$$\begin{aligned} \mathcal{L}_{\mathcal{D}} = & -\log \left(\mathcal{D}(F_S(x), F_V(x)) \right) \\ & - (1 - \mathcal{Y}_{\mathcal{D}}) * \log \left(1 - \mathcal{D}(\mathcal{G}(x), F_V(x)) \right). \end{aligned}$$

The primary challenge in training the detection model is differentiating the naturally occurring prediction disagreement between the service and verification models and the disagreement caused by the attack. As mentioned earlier the trend we observed in our analysis regarding the difference in the divergence ranges between a natural misclassification and an attack allows the detection model to differentiate between the two (refer to Figure 2 in Section VI).

Per Figure 6, during the training process, the reclassification model receives the output of the generator model $(\mathcal{G}(x))$ and verification model $(F_V(x))$ with their cross-entropy loss $(\mathcal{L}(\mathcal{G}(x), F_V(x)))$. It also takes the compatibility label between the service and verification models, *i.e.*, \mathcal{Y}_c , which signifies the correctness of the outputs of these models and their similarity. Using these inputs, we defined the reclassification model's loss as the cross entropy between the output of the reclassification model and \mathcal{Y}_c as:

$$\mathcal{L}_{\mathcal{R}} = - \sum_{c=1}^5 \mathcal{Y}_c * \log \left(\mathcal{R}(\mathcal{G}(x), F_V(x)) \right),$$

where $\mathcal{Y}_c \in \{C1, C2, C3, C4, C5\}$.

After training the attack detection and reclassification models using the proposed GAN, the service provider shares them with the clients. Thus, allowing the clients to independently validate the results of the outsourced workloads.

C. Service Deployment

Without loss of generality, we consider two possibilities for service deployment. In the first approach, the server initiates

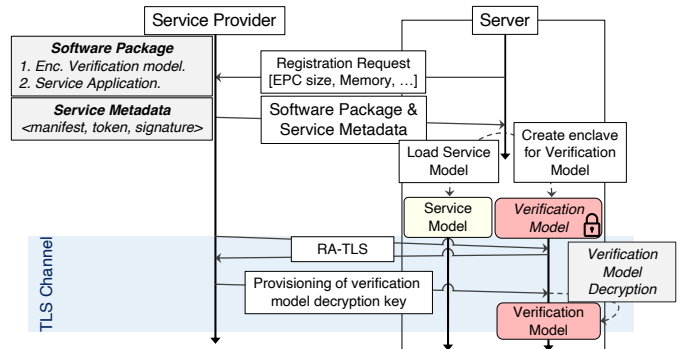


Fig. 7: During the service deployment process, the service provider securely deploys the verification model on a secure enclave on the remote edge server and provisions the decryption key after remote attestation. Thus, guaranteeing the integrity of the verification model.

the deployment process by sending a request to the provider with requisite information about its resources, *e.g.*, EPC size, memory, bandwidth, and the service(s) it is willing to offer. The choice of the service depends on criteria like service demand or resource availability. Alternatively, the service provider initiates the deployment request to a potential server based on service demands in the server's locale. Per Figure 7, we adopt the first approach.

After the final agreement, the provider sends a complete application package to the server. The application package includes the service model, the encrypted verification model, and the service metadata. The service metadata contains application-specific configuration information, which is necessary for the integrity verification of the outsourced application. In particular, for Intel SGX, the metadata contains a `.manifest.sgx` file for configuring the secure application environment by the SGX SDK along with a `.token` and a `.sig` file, which SGX uses to verify the integrity of the enclave-loaded application and files. The server then initiates a secure enclave for loading the encrypted verification model. It then establishes an RA-TLS channel [55] with the service provider for provisioning the application decryption key into the secure enclave. Thus, allowing the enclave to decrypt the verification model.

The service provider shares enclave information, such as $\langle \text{MR_ENCLAVE}, \text{MR_SIGNER}, \text{ISV_PROD}, \text{ISV_SVN} \rangle$ with the clients, enabling them to verify the chain of trust during the remote attestation process (*i.e.*, RA-TLS) at the service outsourcing step. The provider generates these values while creating the SGX-supported application and shares them with the client when the application is downloaded. The RA-TLS protocol helps the client trust the output of the verification model running in the enclave.

D. Service Offloading and Execution

For service offloading, the client starts by discovering the servers that offer the service and have sufficient resources. If the service discovery fails, the client can either offload the service to the provider or request a server to deploy the

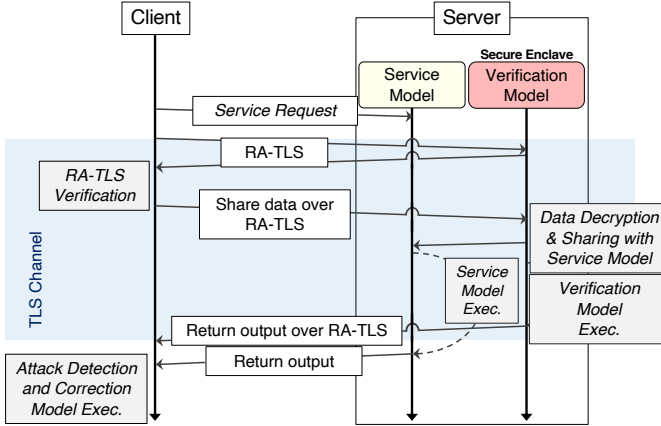


Fig. 8: During service offloading, the client securely shares the data with the secure enclave running the verification model, which in turn shares it with the service model. Thus, ensuring that the verification model has access to trustworthy data.

service. We do not discuss service discovery and assume the client finds a nearby server. Once the client has identified the server, it sends a service request to the server (Figure 8). Considering our threat model, a malicious server can change the data received from the client before sending it to the verification model for verification. Hence, the client first establishes an RA-TLS channel with the enclave to perform remote attestation. The remote attestation process on the client uses $\langle \text{MR_ENCLAVE}, \text{MR_SIGNER}, \text{ISV_PROD}, \text{ISV_SVN} \rangle$ information obtained from the provider to verify the integrity of the respective enclave in terms of its software and configuration. On successful remote attestation, *i.e.*, verifying the chain of trust and ensuring that the client is directly communicating with the secure enclave, the client securely shares the input data with the enclave. The application inside the enclave decrypts the client’s data, shares it with the service model, and executes the verification model. Alternatively, the client can establish a TLS channel with the service model and an RA-TLS channel with the verification model to directly share the data with both. We use the first approach in our experiments.

After completing the offloaded service, the service and verification models return their outputs to the client. Note that the communication between the client and the secure enclave is protected through the established RA-TLS channel. The service model can either set up a secure connection to the client and securely share the result or use an insecure channel. The client then uses Fides’ detection and re-classification pipeline on the outputs of the service and verification models to verify the correctness of outsourced service and detect potential attacks.

VI. EXPERIMENTS

In this Section, we review our benchmark datasets and models and elaborate on our system and experiment setup. We first analyze the similarity of the service and verification models pre- and post-attack and share our observations, which confirms the rationale behind our design. Finally, we assess

TABLE I: Accuracy of service and verification models.

		ResNet	DenseNet	EfficientNet
CIFAR-10	Service	93.77%	94.93%	96.74%
	Verification	93.38%	95.30%	96.91%
CIFAR-100	Service	76.99%	78.69%	83.79%
	Verification	77.31%	76.13%	83.41%
ImageNet	Service	73.01%	73.32%	79.73%
	Verification	70.65%	69.74%	72.16%

the efficacy of Fides in detecting and re-classifying attacks, followed by system performance analysis.

A. Data and Models

We evaluated Fides using datasets of various complexities:

- CIFAR-10 consists of 60K color images (32×32 pixels) with 10 classes and 6K images per class. There are 50000 training and 10000 test images [56].
- CIFAR-100 features 100 classes with 600 images per class with pixels resolution of 32×32 . There are 50000 training and 10000 test images [57].
- ImageNet-1K contains about 1.3M annotated images (about 1.28M training, 50K validation, and 100K test images), grouped into 1000 classes [58]. The resolution of images is 469×387 pixels; we cropped these images to 224×224 pixels.

We used three DNN architectures, namely ResNet, DenseNet, and EfficientNet for the image classification application. More specifically, we used ResNet-152 (60.4M parameters), DenseNet-201 (20.2M parameters), and EfficientNet-B7 (66.7M parameters) as the set of service models and ResNet-50 (25.6M parameters), DenseNet-121 (8.1M parameters), and EfficientNet-B0 (5.3M parameters) as their corresponding verification models, respectively. The accuracy of the corresponding service and verification models on the given datasets are tabulated in Table I. Note that the accuracy of the models we used may not reach the reported accuracy in their respective papers. However, our goal is to use them in developing a result validation mechanism for outsourced ML workload. While we used a similar architecture for each service and verification model pair, it is possible to use different architectures.

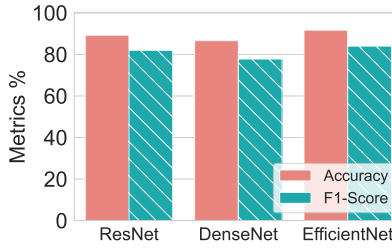
For our GAN framework, we adopted the fully trained service model (architecture and parameter weights) as the generator model and further extended it by adding four extra fully connected layers. The additional layers take the learned decision boundary of the service model at the beginning of the training process and fine-tune the generator model, aiming to craft stronger attack outputs. For the attack detection and re-classification models, we used two lightweight fully connected neural networks, each containing three hidden layers containing 128, 256, and 128 neurons per hidden layer.

B. System and Experiments Setup

We evaluated our framework on a server with an Intel Xeon Platinum 8352Y processor with a base clock speed of 2.20 GHz and 256 GB RAM. The server’s processor is a 3rd generation Xeon processor (*i.e.*, Ice Lake series) with 64 GB EPC. The SGX drivers are in-kernel drivers and were



(a) Detection accuracy on CIFAR-10.



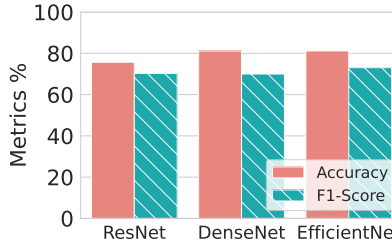
(b) Detection accuracy on CIFAR-100.



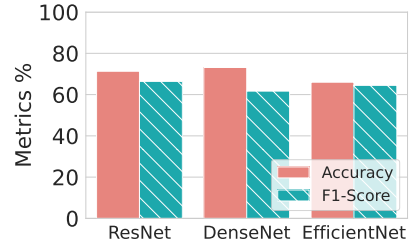
(c) Detection accuracy on ImageNet.



(d) Re-classification accuracy on CIFAR-10.



(e) Re-classification accuracy on CIFAR-100.



(f) Re-classification accuracy on ImageNet.

Fig. 9: Fides' attack detection and re-classification models' performance across all datasets and architecture combinations. The results suggest a direct correlation between the accuracy of the service model and the accuracy of the detection and re-classification models.

implemented using Gramine OS v1.2. We used three classes of consumer processors, namely a mobile class device with a Snapdragon 765G processor, an IoT class device with an ARM Cortex-A72 processor, and an X86 consumer class device with an AMD Ryzen 5 processor.

C. Verification Efficacy Analysis

We evaluated the attack detection and re-classification model's performance in terms of accuracy and F1-score. In doing so, we built a test dataset by randomly selecting an average of 9000 samples from each dataset and applying the attacks we described in Section III-B. We applied the attacks either on the service models' outputs of the 9000 samples (for naive and advanced attacks), input samples (for adversarial example attack), or the service model itself (for Trojan attack). We also included the output of the legitimate service models on the 9000 samples to the test dataset to represent the no-attack scenario. In our experiments, the accuracies we reported for the re-classification models are of the detected samples. Note that running the standalone re-classification models on all the generated attack samples (including the undetected ones) results in higher accuracies than those we discuss below.

For the attack detection and re-classification models, we devised two variants—one that uses the soft labels of the service and verification models as the input features and another one that uses the cross-entropy loss measurement as the input feature. Using the loss measurement enables the detection and re-classification models to utilize the divergence trends we discussed earlier while using soft labels allows the models to learn additional patterns, beyond the divergence trends.

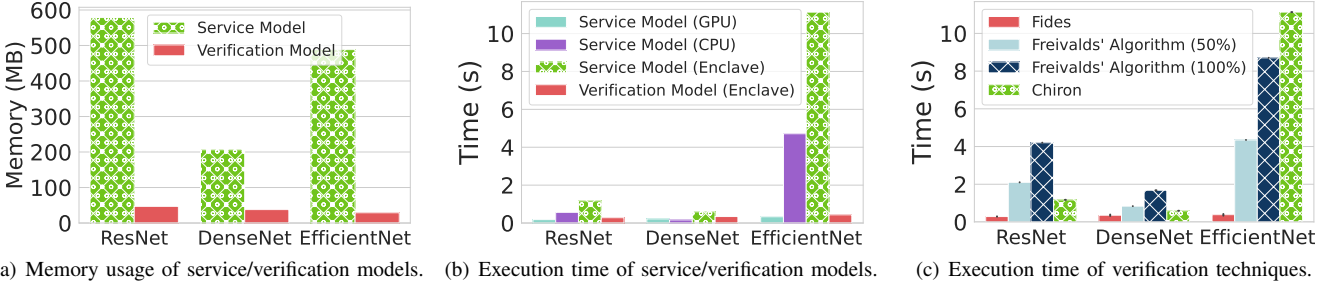
Figure 9 represents the accuracy and F1-Score of the loss-based attack detection and re-classification models across all architectures and datasets. We measured the attack detection

accuracy across all attack scenarios, *i.e.*, from the naive to advanced and well-known attacks. Table II tabulates the attack detection accuracy and F1-score for each attack type. These results show that the attack detection models on average achieve an accuracy of 91.15% across all architectures and datasets and the re-classification models achieve an average accuracy of 80%. More specifically, using EfficientNet for CIFAR-10 results in the best attack detection and re-classification performance (Figures 9(a) and 9(d)). However, increasing the dataset complexity, from CIFAR-10 to ImageNet, slightly reduced the attack detection accuracy with a more moderate impact on the re-classification accuracy (Figures 9(c) and 9(f)). Such behavior is expected as the accuracy of the service and verification models for ImageNet are lower than CIFAR-10 and CIFAR-100 accuracies across all architectures (Table I).

For cases like ImageNet where the accuracy of the service and verification models are (on average) 75.24% and 70.85%, the attack detection accuracy is still higher than 87%, showing that the detection models were successfully identifying attacks where the service model and verification model disagree (the non-trivial scenarios). One can also observe that the performance of the detection and re-classification models are correlated to the service model's accuracy—the more accurate the service model, the more accurate the attack detection and re-classification models. Finally, from our primary investigations, we observed that both loss-based and soft labels-based variants of the attack detection and re-classification models achieve similar performance in terms of accuracy and F1-Score.

D. System Performance Analysis

We also ran a set of experiments to assess Fides's system performance in terms of execution time and memory (Figures 10 and 11). We used the ImageNet dataset in all



(a) Memory usage of service/verification models.

(b) Execution time of service/verification models.

(c) Execution time of verification techniques.

Fig. 10: Evaluation of Fides' server-side performance in terms of memory and execution time on the server.

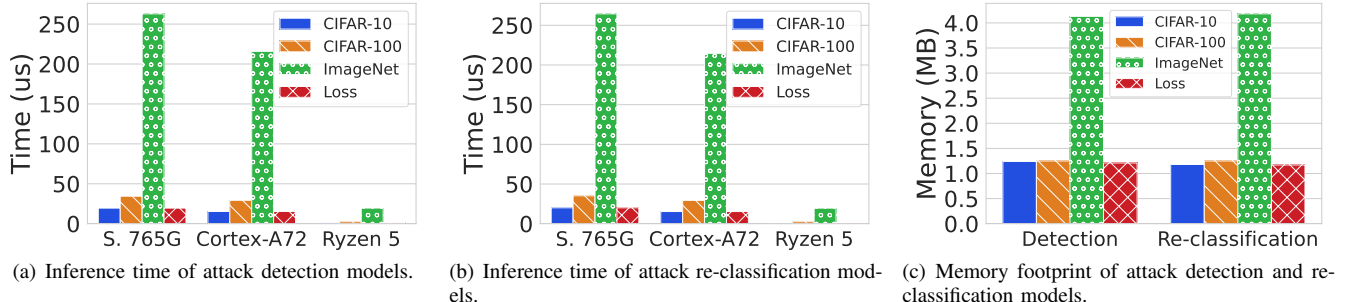


Fig. 11: The number of input features for various datasets impacts the attack detection and re-classification model's performance. Using loss (cross-entropy) for attack detection and re-classification outperforms others due to the smaller feature size.

TABLE II: Attack detection accuracy per attack type.

		ResNet	DenseNet	EfficientNet
CIFAR-10	Accuracy	95.09%	96.59%	97.91%
	Advanced	95.29%	96.75%	98.25%
	FGSM / PGD	89.08%	95.53%	96.06%
	Backdoor	87.92%	88.7%	82.23%
CIFAR-100	Accuracy	94.86%	96.48%	97.88%
	Advanced	95.05%	96.64%	98.22%
	FGSM / PGD	89.25%	95.43%	96.08%
	Backdoor	87.75%	88.95%	84.20%
ImageNet	Accuracy	91.57%	90.19%	92.40%
	Advanced	86.62%	82.90%	88.16%
	FGSM / PGD	94.48%	95.63%	95.21%
	Backdoor	91.90%	93.49%	86.09%
F1-Score	Accuracy	91.76%	90.59%	92.57%
	Advanced	87.52%	84.68%	88.88%
	FGSM / PGD	94.44%	95.58%	95.18%
	Backdoor	92.04%	93.49%	86.09%
F1-Score	Naive	79.41%	77.84%	77.84%
	Advanced	78.31%	77.54%	74.89%
	FGSM / PGD	80.41%	78.71%	79.53%
	Backdoor	80.61%	82.41%	85.25%
F1-Score	Naive	75.15%	72.24%	81.97%
	Advanced	74.94%	72.24%	75.53%
	FGSM / PGD	76.03%	73.03%	73.42%
	Backdoor	79.1%	80.06%	81.25%

architectures for assessing the memory consumption of the server-side components as ImageNet has the most number of classes—the worst-case scenario. Figure 10(a) shows that the GDTL process resulted in a smaller verification model with a significantly smaller memory footprint. This is crucial for deploying real applications on resource-constrained edge servers. We note that the compression ratio may vary across

different models depending on the architecture. Figure 5 (Section V-A) shows the accuracy and the time taken by GDTL when compared to fine tuning (transfer learning) and distillation from scratch. GDTL performed the best accounting for both parameters.

We compared the secure execution of the service and verification models with the insecure service model on CPU and GPU. Figure 10(b) demonstrates that the secure execution of the verification model for ResNet and EfficientNet architectures takes far less than the secure and insecure execution of their service models. For DenseNet, the verification model only takes 0.178 seconds more than the insecure service model but it is still faster than the secure execution of the service model, which we attribute to the DenseNet smaller compression rate. The secure execution of the verification models is marginally slower than GPU executions (worst case 130 milliseconds for DenseNet), which is expected.

We also compared the system performance of Fides with two other techniques—Slalom [26] and Chiron [32]. We selected Slalom as it outperforms other solutions in terms of validation of outsourced ML workloads and selected Chiron due to its similarity with Fides in running the entire model in a TEE. For Slalom, we only implemented its verification process, which uses Freivalds' algorithm to verify the matrix multiplication operations of each linear layer. Considering the probabilistic nature of the verification process in Slalom, we benchmark the verification of 50% and 100% of the service model's matrix multiplications per architecture. We did not include the time of ECALL and OCALL operations (entering

and exiting the enclave), which will result in a large latency overhead considering the frequency of these operations in Slalom. Per Figure 10(c), Fides outperforms other techniques in terms of validation time. It achieves a $1.73\times$ to $25.7\times$ speed-up compared to Chiron and a $4.8\times$ to $26.4\times$ speed-up compared to verification based on Freivalds’ algorithm for 100% of the matrices. This is in part due to the sequential execution of the Freivalds’ algorithm in our experiment. Note that the speed-up in both cases increases with the increase in the size of the verification model.

Given the constrained nature of clients’ devices, we evaluated the performance of the attack detection and re-classification models on several consumer-grade device classes. Figures 11(a) and 11(b) show the elapsed time of running these models on an Internet of Things device (ARM Cortex-A72), a smartphone (Snapdragon 765G), and a personal desktop (AMD Ryzen 5). One can observe the negligible overhead of these models on clients; less than 260 microseconds in the worst case. Our analyses show that the performance of these models is highly correlated to the size of their input features when using soft labels as the input. For instance, detecting an attack on ImageNet with 1000 classes takes (on average) $13.47\times$ longer than detecting the same attack on CIFAR-10 with 10 classes. The same behavior can be observed from attack re-classification models. However, the loss-based detection and re-classification models show significant improvement in the execution time—only 0.076% of the original latency in the case of ImageNet soft labels. This is primarily due to the independence of the model’s input size to the number of the service model’s classes when using cross-entropy loss value as the input feature. It is worth mentioning that the added overhead of loss calculation for the two input vectors is negligible. Figure 11(c) shows the memory footprint of different detection and re-classification models. The memory footprint falls within a similar range for CIFAR-10, CIFAR-100, and the loss-based solutions but increases significantly for ImageNet. It is primarily due to the smaller input layers for CIFAR-10, CIFAR-100, and loss-based solution, when compared with ImageNet’s larger input layer.

VII. RELATED WORK

The defenses against integrity violations in machine learning models during inference can be classified into three categories.

Cryptographic defences include solutions like multi-party computation [16]–[19], proof-based systems [20]–[22], various constructions of homomorphic encryption [22]–[25]. While the primary goal of multi-party computation is protecting data privacy, this technique offers a degree of verifiability. Similarly, solutions based on homomorphic encryption provide verifiability by virtue of protecting the data. For instance, one secure inference operation of the ResNet50 model using homomorphic encryption on customized hardware takes about 970 seconds compared to only 100 milliseconds for the same operation on non-encrypted data [59].

In contrast to these schemes, proof-based systems, *e.g.*, interactive and zero-knowledge succinct non-interactive ar-

gument of knowledge (zk-SNARK), have been extensively used for verifiable ML [20], [21], [60]–[64]. The proof-based solutions, although theoretically more representative of verification, require significant computation by the prover [21] and do not scale for large ML models with many convolution layers [65]. For instance, generating proof for the VGG16 model with 16 layers and a decision tree with 23 levels take 88.3 seconds and 250 seconds, respectively [60], [63]. Moreover, the authors in [26] have shown that the best proof-based verifiable ML scheme is roughly 200 times slower when compared with running the entire model in a TEE.

TEE-based defenses has been used extensively in ML security and privacy, where confidentiality, privacy, and verifiability are paramount [26], [29], [66], [67]. In this domain, the main body of the literature aims at the efficient and secure execution of advanced models and large datasets in TEEs with small enclave page cache (EPC) [31], [68], [69]. These frameworks generally suggest partial outsourcing, in which a subset of the layers will be outsourced for secure execution. More specifically, the authors in [68], [69] suggested running the last few layers in one or multiple parallel enclaves and the rest of the layers by the client. Alternative approaches proposed running the linear layers in a secure enclave and the remaining layers outside in insecure memory and verifying them using Freivalds’ algorithm [26].

Attack Specific Defences could be designed to defend against backdoor attacks in the training phase [70]–[73] by identifying and eliminating the updates or samples that are out-of-distribution. Since adversarial sample attacks take place in inference phase, the defenses against adversarial samples can take several different approaches, such as training discriminators to capture the difference between the training data and adversarial samples [74]–[76] or relying on invariance in the feature map and activation caused due to adversarial behavior [77]–[79].

Fides aims to overcome the shortcomings of these solutions by deploying a validation system, which relies on a significantly smaller verification model’s posterior information to validate the prediction of service model. Fides aims to be highly parallelizable in deployment while being adaptable to already deployed MLaaS models. Fides also aims to make the defense attack methodology agnostic.

VIII. CONCLUSION

We introduced Fides—a framework for output verification of outsourced ML workloads. Fides features a Greedy model distillation technique. GDTL process gradually unfreezes the layers of an off-the-shelf model for distillation-based fine-tuning. Along with deploying the service model, the provider also securely deploys the verification model in a TEE on the server. The client then offloads the ML workload to the server by sharing its data with the service and verification models. Fides also features client-side neural networks for attack detection and re-classification, which are trained via our proposed GAN framework. Our rigorous evaluation using multiple datasets and neural network architectures shows Fides

to be superior to the existing solutions in system performance—a $1.73\times$ to $26.4\times$ speed-up and achieves up to 98% attack detection and re-classification accuracy. In the future, we will extend the GDTL pipeline to an ensemble of service models and analyzing Fides’ performance on other ML models.

REFERENCES

[1] Q. Zhang, Q. Zhang, W. Shi, and H. Zhong, “Distributed collaborative execution on the edges and its application to amber alerts,” *IEEE Internet of Things Journal*, vol. 5, no. 5, pp. 3580–3593, 2018.

[2] S. Liu, L. Liu, J. Tang, B. Yu, Y. Wang, and W. Shi, “Edge computing for autonomous driving: Opportunities and challenges,” *Proceedings of the IEEE*, vol. 107, no. 8, pp. 1697–1716, 2019.

[3] P. P. Ray, D. Dash, and D. De, “Edge computing for internet of things: A survey, e-healthcare case study and future direction,” *Journal of Network and Computer Applications*, vol. 140, pp. 1–22, 2019.

[4] Y. Siriwardhana, P. Porambage, M. Liyanage, and M. Ylianttila, “A survey on mobile augmented reality with 5g mobile edge computing: Architectures, applications, and technical aspects,” *IEEE Communications Surveys & Tutorials*, vol. 23, no. 2, pp. 1160–1192, 2021.

[5] R. Tourani, S. Srikanthswara, S. Misra, R. Chow, L. Yang, X. Liu, and Y. Zhang, “Democratizing the edge: A pervasive edge computing framework,” *arXiv preprint arXiv:2007.00641*, 2020.

[6] Q. Liu, P. Li, W. Zhao, W. Cai, S. Yu, and V. C. Leung, “A survey on security threats and defensive techniques of machine learning: A data driven view,” *IEEE access*, vol. 6, pp. 12 103–12 117, 2018.

[7] M. Nasr, R. Shokri, and A. Houmansadr, “Comprehensive privacy analysis of deep learning: Passive and active white-box inference attacks against centralized and federated learning,” in *2019 IEEE symposium on security and privacy (SP)*. IEEE, 2019, pp. 739–753.

[8] R. Tang, M. Du, N. Liu, F. Yang, and X. Hu, “An embarrassingly simple approach for trojan attack in deep neural networks,” in *Proceedings of the 26th ACM SIGKDD International Conference on Knowledge Discovery & Data Mining*, 2020, pp. 218–228.

[9] B. Liu, M. Ding, S. Shaham, W. Rahayu, F. Farokhi, and Z. Lin, “When machine learning meets privacy: A survey and outlook,” *ACM Computing Surveys (CSUR)*, vol. 54, no. 2, pp. 1–36, 2021.

[10] X. Zhang, Z. Zhang, S. Ji, and T. Wang, “Trojaning language models for fun and profit,” in *2021 IEEE European Symposium on Security and Privacy (EuroS&P)*. IEEE, 2021, pp. 179–197.

[11] S. Cheng, Y. Liu, S. Ma, and X. Zhang, “Deep feature space trojan attack of neural networks by controlled detoxification,” in *Proceedings of the AAAI Conference on Artificial Intelligence*, vol. 35, no. 2, 2021, pp. 1148–1156.

[12] F. Tramèr, R. Shokri, A. San Joaquin, H. Le, M. Jagielski, S. Hong, and N. Carlini, “Truth serum: Poisoning machine learning models to reveal their secrets,” in *Proceedings of the 2022 ACM SIGSAC Conference on Computer and Communications Security*, 2022, pp. 2779–2792.

[13] N. Papernot, P. McDaniel, and I. Goodfellow, “Transferability in machine learning: from phenomena to black-box attacks using adversarial samples,” *arXiv preprint arXiv:1605.07277*, 2016.

[14] G. Tao, S. Ma, Y. Liu, and X. Zhang, “Attacks meet interpretability: Attribute-steered detection of adversarial samples,” *Advances in Neural Information Processing Systems*, vol. 31, 2018.

[15] Y. Yao, H. Li, H. Zheng, and B. Y. Zhao, “Latent backdoor attacks on deep neural networks,” in *Proceedings of the 2019 ACM SIGSAC conference on computer and communications security*, 2019, pp. 2041–2055.

[16] Z. Huang, W.-j. Lu, C. Hong, and J. Ding, “Cheetah: Lean and fast secure two-party deep neural network inference.” *IACR Cryptol. ePrint Arch.*, vol. 2022, p. 207, 2022.

[17] E. Sothiwat, L. Zhen, Z. Li, and C. Zhang, “Partially encrypted multi-party computation for federated learning,” in *2021 IEEE/ACM 21st International Symposium on Cluster, Cloud and Internet Computing (CCGrid)*. IEEE, 2021, pp. 828–835.

[18] S. Yuan, M. Shen, I. Mironov, and A. C. Nascimento, “Practical, label private deep learning training based on secure multiparty computation and differential privacy,” *Cryptology ePrint Archive*, 2021.

[19] B. Knott, S. Venkataraman, A. Hannun, S. Sengupta, M. Ibrahim, and L. van der Maaten, “Crypten: Secure multi-party computation meets machine learning,” *Advances in Neural Information Processing Systems*, vol. 34, pp. 4961–4973, 2021.

[20] Z. Ghodsi, T. Gu, and S. Garg, “Safetynets: Verifiable execution of deep neural networks on an untrusted cloud,” *Advances in Neural Information Processing Systems*, vol. 30, 2017.

[21] S. Lee, H. Ko, J. Kim, and H. Oh, “vcnn: Verifiable convolutional neural network based on zk-snarks,” *Cryptology ePrint Archive*, 2020.

[22] A. Madi, R. Sirdey, and O. Stan, “Computing neural networks with homomorphic encryption and verifiable computing,” in *International Conference on Applied Cryptography and Network Security*. Springer, 2020, pp. 295–317.

[23] C. Niu, F. Wu, S. Tang, S. Ma, and G. Chen, “Toward verifiable and privacy preserving machine learning prediction,” *IEEE Transactions on Dependable and Secure Computing*, 2020.

[24] G. Xu, H. Li, H. Ren, J. Sun, S. Xu, J. Ning, H. Yang, K. Yang, and R. H. Deng, “Secure and verifiable inference in deep neural networks,” in *Annual Computer Security Applications Conference*, 2020, pp. 784–797.

[25] D. Natarajan, W. Dai, and R. Dreslinski, “Chex-mix: Combining homomorphic encryption with trusted execution environments for two-party oblivious inference in the cloud,” *Cryptology ePrint Archive*, 2021.

[26] F. Tramer and D. Boneh, “Slalom: Fast, verifiable and private execution of neural networks in trusted hardware,” *arXiv preprint arXiv:1806.03287*, 2018.

[27] K. Grover, S. Tople, S. Shinde, R. Bhagwan, and R. Ramjee, “Privado: Practical and secure dnn inference with enclaves,” *arXiv preprint arXiv:1810.00602*, 2018.

[28] A. Moubayed, M. Injadat, A. Shami, and H. Lutfiyya, “Dns typo-squatting domain detection: A data analytics and machine learning based approach,” in *2018 IEEE Global Communications Conference (GLOBECOM)*, 2018, pp. 1–7.

[29] H. Hashemi, Y. Wang, and M. Annavaram, “Darknight: An accelerated framework for privacy and integrity preserving deep learning using trusted hardware,” in *MICRO-54: 54th Annual IEEE/ACM International Symposium on Microarchitecture*, 2021, pp. 212–224.

[30] G. Hinton, O. Vinyals, J. Dean *et al.*, “Distilling the knowledge in a neural network,” *arXiv preprint arXiv:1503.02531*, vol. 2, no. 7, 2015.

[31] F. Mo, H. Haddadi, K. KATEVAS, E. Marin, D. Perino, and N. Kourtellis, “Ppfl: privacy-preserving federated learning with trusted execution environments,” in *Proceedings of the 19th Annual International Conference on Mobile Systems, Applications, and Services*, 2021, pp. 94–108.

[32] T. Hunt, C. Song, R. Shokri, V. Shmatikov, and E. Witchel, “Chiron: Privacy-preserving machine learning as a service,” *arXiv preprint arXiv:1803.05961*, 2018.

[33] K. He, X. Zhang, S. Ren, and J. Sun, “Deep residual learning for image recognition,” in *Proceedings of the IEEE conference on computer vision and pattern recognition*, 2016, pp. 770–778.

[34] G. Huang, Z. Liu, L. Van Der Maaten, and K. Q. Weinberger, “Densely connected convolutional networks,” in *Proceedings of the IEEE conference on computer vision and pattern recognition*, 2017, pp. 4700–4708.

[35] M. Tan and Q. Le, “Efficientnet: Rethinking model scaling for convolutional neural networks,” in *International conference on machine learning*. PMLR, 2019, pp. 6105–6114.

[36] N. Asokan, J.-E. Ekberg, K. Kostiainen, A. Rajan, C. Rozas, A.-R. Sadeghi, S. Schulz, and C. Wachsmann, “Mobile trusted computing,” *Proceedings of the IEEE*, vol. 102, no. 8, pp. 1189–1206, 2014.

[37] M. Sabt, M. Achemlal, and A. Bouabdallah, “Trusted execution environment: What it is, and what it is not,” in *2015 IEEE Trustcom/BigDataSE/ISPA*, vol. 1, 2015, pp. 57–64.

[38] V. Costan and S. Devadas, “Intel sgx explained,” *Cryptology ePrint Archive*, 2016.

[39] T. Alves, “Trustzone: Integrated hardware and software security,” *White paper*, 2004.

[40] S. Han, H. Mao, and W. J. Dally, “Deep compression: Compressing deep neural networks with pruning, trained quantization and huffman coding,” *arXiv preprint arXiv:1510.00149*, 2015.

[41] S. Zhou, Y. Wu, Z. Ni, X. Zhou, H. Wen, and Y. Zou, “Dorefa-net: Training low bitwidth convolutional neural networks with low bitwidth gradients,” *arXiv preprint arXiv:1606.06160*, 2016.

[42] C. Zhu, S. Han, H. Mao, and W. J. Dally, “Trained ternary quantization,” *arXiv preprint arXiv:1612.01064*, 2016.

[43] Y. Cheng, D. Wang, P. Zhou, and T. Zhang, “A survey of model compression and acceleration for deep neural networks,” *arXiv preprint arXiv:1710.09282*, 2017.

[44] T. Furlanello, Z. Lipton, M. Tschannen, L. Itti, and A. Anandkumar, “Born again neural networks,” in *International Conference on Machine Learning*. PMLR, 2018, pp. 1607–1616.

[45] H. Bagherinezhad, M. Horton, M. Rastegari, and A. Farhadi, “Label refinery: Improving imagenet classification through label progression,” *arXiv preprint arXiv:1805.02641*, 2018.

[46] S. Hofstätter, S. Althammer, M. Schröder, M. Sertkan, and A. Hanbury, "Improving efficient neural ranking models with cross-architecture knowledge distillation," *arXiv preprint arXiv:2010.02666*, 2020.

[47] G. Ortiz-Jiménez, A. Modas, S.-M. Moosavi-Dezfooli, and P. Frossard, "Optimism in the face of adversity: Understanding and improving deep learning through adversarial robustness," *Proceedings of the IEEE*, vol. 109, no. 5, pp. 635–659, 2021.

[48] J. Maroto, G. Ortiz-Jiménez, and P. Frossard, "On the benefits of knowledge distillation for adversarial robustness," *arXiv preprint arXiv:2203.07159*, 2022.

[49] N. Papernot, P. McDaniel, X. Wu, S. Jha, and A. Swami, "Distillation as a defense to adversarial perturbations against deep neural networks," in *2016 IEEE symposium on security and privacy (SP)*. IEEE, 2016, pp. 582–597.

[50] I. J. Goodfellow, J. Shlens, and C. Szegedy, "Explaining and harnessing adversarial examples," *arXiv preprint arXiv:1412.6572*, 2014.

[51] A. Kurakin, I. Goodfellow, S. Bengio *et al.*, "Adversarial examples in the physical world," 2016.

[52] X. Chen, C. Liu, B. Li, K. Lu, and D. Song, "Targeted backdoor attacks on deep learning systems using data poisoning," 2017.

[53] T. Gu, B. Dolan-Gavitt, and S. Garg, "Badnets: Identifying vulnerabilities in the machine learning model supply chain," *arXiv preprint arXiv:1708.06733*, 2017.

[54] L. Yang and A. Shami, "On hyperparameter optimization of machine learning algorithms: Theory and practice," *Neurocomputing*, vol. 415, pp. 295–316, 2020.

[55] T. Knauth, M. Steiner, S. Chakrabarti, L. Lei, C. Xing, and M. Vij, "Integrating remote attestation with transport layer security," *arXiv preprint arXiv:1801.05863*, 2018.

[56] A. Krizhevsky, V. Nair, and G. Hinton, "Cifar-10 (canadian institute for advanced research)." [Online]. Available: <http://www.cs.toronto.edu/~kriz/cifar.html>

[57] ———, "Cifar-100 (canadian institute for advanced research)." [Online]. Available: <http://www.cs.toronto.edu/~kriz/cifar.html>

[58] J. Deng, W. Dong, R. Socher, L.-J. Li, K. Li, and L. Fei-Fei, "Imagenet: A large-scale hierarchical image database," in *Conference on computer vision and pattern recognition*. IEEE, 2009, pp. 248–255.

[59] B. Reagen, W.-S. Choi, Y. Ko, V. T. Lee, H.-H. S. Lee, G.-Y. Wei, and D. Brooks, "Cheetah: Optimizing and accelerating homomorphic encryption for private inference," in *2021 IEEE International Symposium on High-Performance Computer Architecture*. IEEE, 2021, pp. 26–39.

[60] T. Liu, X. Xie, and Y. Zhang, "Zkcnn: Zero knowledge proofs for convolutional neural network predictions and accuracy," in *Proceedings of the 2021 ACM SIGSAC Conference on Computer and Communications Security*, 2021, pp. 2968–2985.

[61] N. Singh, P. Dayama, and V. Pandit, "Zero knowledge proofs towards verifiable decentralized ai pipelines," *Cryptology ePrint Archive*, 2021.

[62] D. Demirel, L. Schabhüser, and J. Buchmann, "Proof and argument based verifiable computing," in *Privately and Publicly Verifiable Computing Techniques*. Springer, 2017, pp. 13–22.

[63] J. Zhang, Z. Fang, Y. Zhang, and D. Song, "Zero knowledge proofs for decision tree predictions and accuracy," in *Proceedings of the 2020 ACM SIGSAC Conference on Computer and Communications Security*, 2020, pp. 2039–2053.

[64] J. Weng, J. Weng, G. Tang, A. Yang, M. Li, and J.-N. Liu, "pvcnn: Privacy-preserving and verifiable convolutional neural network testing," *arXiv preprint arXiv:2201.09186*, 2022.

[65] L. Zhao, Q. Wang, C. Wang, Q. Li, C. Shen, and B. Feng, "Veriml: Enabling integrity assurances and fair payments for machine learning as a service," *IEEE Transactions on Parallel and Distributed Systems*, vol. 32, no. 10, pp. 2524–2540, 2021.

[66] A. Gangal, M. Ye, and S. Wei, "Hybridtee: Secure mobile dnn execution using hybrid trusted execution environment," in *2020 Asian Hardware Oriented Security and Trust Symposium (AsianHOST)*. IEEE, 2020, pp. 1–6.

[67] C. Dong, J. Weng, Y. Tong, J.-N. Liu, A. Yang, Y. Cheng, and S. Hu, "Fusion: Efficient and secure inference resilient to malicious server and curious clients," *arXiv preprint arXiv:2205.03040*, 2022.

[68] F. Mo, A. S. Shamsabadi, K. Katevas, S. Demetriadis, I. Leontiadis, A. Cavallaro, and H. Haddadi, "Darknetz: towards model privacy at the edge using trusted execution environments," in *Proceedings of the International Conference on Mobile Systems, Applications, and Services*, 2020, pp. 161–174.

[69] A. Kumar, R. Tourani, M. Vij, and S. Srikantewara, "Sclera: A framework for privacy-preserving mlaas at the pervasive edge," in *International Conference on Pervasive Computing and Communications Workshops and other Affiliated Events*. IEEE, 2022, pp. 175–180.

[70] T. D. Nguyen, P. Rieger, R. De Viti, H. Chen, B. B. Brandenburg, H. Yalame, H. Möllering, H. Fereidooni, S. Marchal, M. Miettinen *et al.*, "{FLAME}: Taming backdoors in federated learning," in *31st USENIX Security Symposium (USENIX Security 22)*, 2022, pp. 1415–1432.

[71] M. Charikar, J. Steinhardt, and G. Valiant, "Learning from untrusted data," in *Proceedings of the 49th Annual ACM SIGACT Symposium on Theory of Computing*, 2017, pp. 47–60.

[72] N. Peri, N. Gupta, W. R. Huang, L. Fowl, C. Zhu, S. Feizi, T. Goldstein, and J. P. Dickerson, "Deep k-nn defense against clean-label data poisoning attacks," in *Computer Vision–ECCV 2020 Workshops: Glasgow, UK, August 23–28, 2020, Proceedings, Part I 16*. Springer, 2020, pp. 55–70.

[73] B. Tran, J. Li, and A. Madry, "Spectral signatures in backdoor attacks," *Advances in neural information processing systems*, vol. 31, 2018.

[74] F. Zuo and Q. Zeng, "Exploiting the sensitivity of l2 adversarial examples to erase-and-restore," in *Proceedings of the 2021 ACM Asia Conference on Computer and Communications Security*, 2021, pp. 40–51.

[75] K. Lee, K. Lee, H. Lee, and J. Shin, "A simple unified framework for detecting out-of-distribution samples and adversarial attacks," *Advances in neural information processing systems*, vol. 31, 2018.

[76] H. F. Eniser, M. Christakis, and V. Wüstholtz, "Raid: Randomized adversarial-input detection for neural networks," *arXiv preprint arXiv:2002.02776*, 2020.

[77] J. Lu, T. Issaranon, and D. Forsyth, "Safetynet: Detecting and rejecting adversarial examples robustly," in *Proceedings of the IEEE international conference on computer vision*, 2017, pp. 446–454.

[78] S. Pertigkiozoglu and P. Maragos, "Detecting adversarial examples in convolutional neural networks," *arXiv preprint arXiv:1812.03303*, 2018.

[79] J. H. Metzen, T. Genewein, V. Fischer, and B. Bischoff, "On detecting adversarial perturbations," *arXiv preprint arXiv:1702.04267*, 2017.

APPENDIX A
COMPLEMENTARY RESULTS

TABLE III: Entropy Analysis of Jeffreys Divergence (JD) and Wasserstein Metric (WM) for cases that service and verification models predictions are identical (Case A) post-attack.

		Case A		
		ResNet	DenseNet	EfficientNet
CIFAR-10	WM	Pre-attack	0.0027 \pm 0.002	0.0013 \pm 0.001
		Post-attack	2.08 \pm 1.89	2.44 \pm 1.98
	JD	Pre-attack	0.009 \pm 0.009	0.004 \pm 0.0001
		Post-attack	13.09 \pm 5.3	13.09 \pm 4.37
CIFAR-100	WM	Pre-attack	0.037 \pm 0.024	0.035 \pm 0.034
		Post-attack	6.63 \pm 2.16	6.74 \pm 2.1
	JD	Pre-attack	0.03 \pm 0.0293	0.037 \pm 0.035
		Post-attack	9.53 \pm 3.98	10.25 \pm 4.12
ImageNet	WM	Pre-attack	0.19 \pm 0.18	0.35 \pm 0.31
		Post-attack	7.59 \pm 5.15	7.04 \pm 4.66
	JD	Pre-attack	0.035 \pm 0.032	0.065 \pm 0.06
		Post-attack	3.96 \pm 2.16	3.31 \pm 1.82

TABLE IV: Entropy Analysis of Jeffreys Divergence (JD) and Wasserstein Metric (WM) for cases that service and verification models predictions are different (Case B) post-attack.

		Case B		
		ResNet	DenseNet	EfficientNet
CIFAR-10	WM	Pre-attack	1.66 \pm 0.43	1.76 \pm 0.45
		Post-attack	0.79 \pm 0.46	0.80 \pm 0.53
	JD	Pre-attack	4.76 \pm 1.99	4.83 \pm 2.09
		Post-attack	1.75 \pm 1.36	1.64 \pm 1.21
CIFAR-100	WM	Pre-attack	5.37 \pm 1.61	5.27 \pm 1.49
		Post-attack	3.73 \pm 1.9	3.85 \pm 1.79
	JD	Pre-attack	4.77 \pm 1.69	5.67 \pm 0.035
		Post-attack	3.67 \pm 2.523	4.50 \pm 2.99
ImageNet	WM	Pre-attack	5.68 \pm 2.42	5.29 \pm 2.44
		Post-attack	4.68 \pm 2.38	4.35 \pm 2.16
	JD	Pre-attack	1.30 \pm 0.56	1.20 \pm 0.50
		Post-attack	1.07 \pm 0.58	1.03 \pm 0.54